ISSN 0030-400X, Optics and Spectroscopy, 2007, Vol. 103, No. 2, pp. 231–236. © Pleiades Publishing, Ltd., 2007.

QUANTUM OPTICS AND PRECISION MEASUREMENTS, APPLICATIONS TO GRAVITATIONAL EXPERIMENTS

Optimized Interferometry with Gaussian States[1]

S. Olivares and M. G. A. Paris

Dipartimento di Fisica dell'Università degli Studi, Milano, Italia

e-mail: Stefano.Olivares@mi.infn.it

Received October 12, 2006

Abstract—We revisit Mach–Zehnder interferometry using a suitable phase-space analysis and present a rigorous optimization of the sensitivity in realistic condition, i.e., for Gaussian input states, and taking into account nonunit quantum efficiency in the detection stage. The working regime of the interferometer is optimized at fixed input energy versus the squeezing phases and amplitudes as well as the distribution of squeezing in the two input signals. For ideal detection we find the known result that the squeezing resource allows to beat the shot-noise limit. For nonunit detection efficiency, we show that for fixed input energy one can always optimize the squeezing fraction in order to enhance the sensitivity with respect to the case of no squeezing, even in cases when one cannot go beyond the shot-noise limit.

PACS numbers: 42.50.St

DOI: 10.1134/S0030400X07080103

1. INTRODUCTION

Fluctuations of some environmental parameter, such as small variations of the refraction index or small displacement induced by weak forces, may lead to a small change in the optical path of a light beam, which can be detected by means of an interferometer measuring the induced phase shift of the radiation field. A figure of merit that one can use to characterize the performances of the interferometer is its sensitivity. In general there are different sources of noise which can limit sensitivity and one of these is due to the detection stage (photon-counting statistics errors), depending on the measurement process and on its quantum efficiency. On the other hand, the sensitivity is ultimately limited by the "standard quantum limit" (SQL), which is somehow related to the Heisenberg uncertainty relation.

The issue of optimizing interferometry has been addressed by several authors. Caves has shown [1, 2] that the main contribution affecting sensitivity is given by the photon-counting statistics error, which can be reduced by "squeezing" the field modes before they enter the interferometer, leading to an improvement of the sensitivity [3]. In turn, the main problem becomes to find out the optimal input states which allow for the most accurate phase shift measurement when the number of detected photon at the output of the interferometer is fixed and the detection quantum efficiency is given [4] or when the interferometer is subjected to some mechanical noise [5]. More generally, phase shift estimation can be addressed by means of information theory considerations using Bayesian analysis [6, 7] or can be seen as a binary decision problem [8]. Indeed, phase estimation is not only related to optical interferometers, but also to matter-wave interferometers [9], such as neutron-based interferometers [6]. Interferometry with path-entangled quantum states (of photons or atoms) has been recently investigated in order to provide unbiased phase estimation with enhanced sensitivity [10, 11].

In this paper we revisit the dynamics of the Mach–Zehnder (MZ) interferometer using a suitable phase-space description when the two-mode input state is Gaussian and, in particular, when the input states are two squeezed coherent states. In this way we are able to present a rigorous optimization of sensitivity over the different input state parameters. We find the optimal working regime of the interferometer versus the squeezing phases and further optimize it with respect to the total squeezing fraction. Moreover, we investigate how squeezing should be distributed between the input states in order to obtain the best performances taking also in account the quantum efficiency at the detection stage. Overall, we obtain a rigorous optimization of the performances of the interferometer, which does not rely on specific assumptions of the amount of impinged energy or squeezing.

The paper is structured as follows: in Section 2 the dynamics of the MZ interferometer is analyzed and its optimal working regime is found out in the case of squeezed input states. The sensitivity of the interferometer is introduced in Section 3 and then investigated for both the cases of ideal (Section 3.1) and real detection (Section 3.2). Some concluding remarks are finally drawn in Section 4.

[1] The text was submitted by the authors in English.

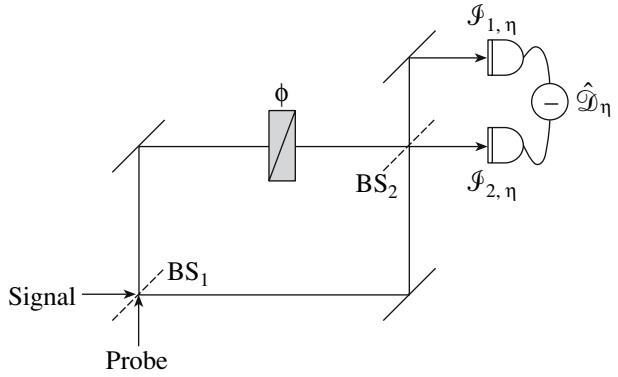

Fig. 1. Sketch of the MZ interferometer: the two modes of the input states are mixed at the balanced beam splitter BS_1 and one of the two outgoing modes undergoes a phase-shift of an amount ϕ before it is mixed again with the other one at the balanced beam splitter BS_2. Finally the difference current $\hat{\mathcal{D}}_\eta = \mathcal{J}_{1,\eta} - \mathcal{J}_{2,\eta}$ is evaluated, η being the quantum efficiency of both detectors.

2. MACH–ZEHNDER INTERFEROMETER DYNAMICS

The scheme of the MZ interferometer sketched in Fig. 1. Here we consider the evolution through the MZ of a bipartite Gaussian state $\varrho_{\rm in}$ described by the characteristic function

$$\chi_{\rm in}(\mathbf{\Lambda}) = \exp\{(-1/2)\mathbf{\Lambda}^T\boldsymbol{\sigma}_{\rm in}\mathbf{\Lambda} + i\mathbf{\Lambda}^T\mathbf{X}_{\rm in}\}, \quad (1)$$

where $\mathbf{\Lambda}^T = (x_1, y_1, x_2, y_2)$, $(\ldots)^T$, being the transposition operation, $\boldsymbol{\sigma}_{\rm in}$ is the 4×4 covariance matrix and $\mathbf{X}_{\rm in}^T = {\rm Tr}[\varrho_{\rm in}(q_1, p_1, q_2, p_2)^T]$, with $q_k = (a_k^\dagger + a_k)/\sqrt{2}$ and $p_k = i(a_k^\dagger - a_k)/\sqrt{2}$, a_k being the kth field mode.

The symplectic matrices associated with the balanced BSs, the mirrors and the phase shifter are given by

$$\mathbf{S}_{\rm BS} = \frac{1}{\sqrt{2}}\left(\begin{array}{c|c} \mathbb{1}_2 & \mathbb{1}_2 \\ \hline -\mathbb{1}_2 & \mathbb{1}_2 \end{array}\right), \quad \mathbf{S}_{\rm M} = \left(\begin{array}{c|c} \mathbf{0} & \mathbb{1}_2 \\ \hline -\mathbb{1}_2 & \mathbf{0} \end{array}\right) \quad (2)$$

and

$$\mathbf{S}_\phi = \left(\begin{array}{c|c} \mathbf{R}_\phi & \mathbf{0} \\ \hline \mathbf{0} & \mathbb{1}_2 \end{array}\right), \quad \mathbf{R}_\phi = \left(\begin{array}{cc} \cos\phi & -\sin\phi \\ \sin\phi & \cos\phi \end{array}\right), \quad (3)$$

$\mathbb{1}_2$ and $\mathbf{0}$ being the 2×2 identity and null matrices, respectively. Since the evolution through the interferometer preserves the Gaussian character of the input, after the characteristic function associated to the state $\varrho_{\rm out}$ after the second BS reads as follows:

$$\chi_{\rm out}(\mathbf{\Lambda}) = \exp\{(-1/2)\mathbf{\Lambda}^T\boldsymbol{\sigma}_{\rm out}\mathbf{\Lambda} + i\mathbf{\Lambda}^T\mathbf{X}_{\rm out}\}, \quad (4)$$

where [12]

$$\boldsymbol{\sigma}_{\rm out} = (\mathbf{S}_{\rm BS}\mathbf{S}_{\rm M}\mathbf{S}_\phi\mathbf{S}_{\rm BS})^T\boldsymbol{\sigma}_{\rm in}(\mathbf{S}_{\rm BS}\mathbf{S}_{\rm M}\mathbf{S}_\phi\mathbf{S}_{\rm BS}) \quad (5)$$

and

$$\mathbf{X}_{\rm out} = (\mathbf{S}_{\rm BS}\mathbf{S}_{\rm M}\mathbf{S}_\phi\mathbf{S}_{\rm BS})^T\mathbf{X}_{\rm in}. \quad (6)$$

By writing the output covariance matrix as

$$\boldsymbol{\sigma}_{\rm out} = \left(\begin{array}{cc|cc} a & c & e & f \\ c & b & g & h \\ \hline e & g & A & C \\ f & h & C & B \end{array}\right), \quad (7)$$

and $\mathbf{X}_{\rm out}^T = (X_1, Y_1, X_2, Y_2)$, we can write the characteristic function in complex notation as follows:

$$\begin{aligned}\chi_{\rm out}(\lambda_1, \lambda_2) = \exp\{&-\mathcal{A}|\lambda_1|^2 - \mathcal{B}|\lambda_2|^2 - \mathcal{C}\lambda_1^2 \\ &- \mathcal{C}^*\lambda_1^{*2} - \mathcal{D}\lambda_2^2 - \mathcal{D}^*\lambda_2^{*2} - \mathcal{E}\lambda_1\lambda_2 - \mathcal{E}^*\lambda_1^*\lambda_2^* \\ &- \mathcal{F}\lambda_1\lambda_2^* - \mathcal{F}^*\lambda_1^*\lambda_2 \\ &+ i[\mathcal{U}^*\lambda_1 + \mathcal{U}\lambda_1^* + \mathcal{V}^*\lambda_2 + \mathcal{V}\lambda_2^*]\}\end{aligned} \quad (8)$$

with

$$\mathcal{A} = \frac{1}{2}(a+b), \quad \mathcal{B} = \frac{1}{2}(A+B), \quad (9)$$

$$\mathcal{C} = \frac{1}{4}(a-b+2ic), \quad \mathcal{D} = \frac{1}{4}(A-B+2iC), \quad (10)$$

$$\begin{aligned}\mathcal{E} &= \frac{1}{2}[e-h+i(f+g)], \\ \mathcal{F} &= \frac{1}{2}[e+h+i(f-g)],\end{aligned} \quad (11)$$

$$\mathcal{U} = \frac{1}{\sqrt{2}}(X_1 + iY_1), \quad \mathcal{V} = \frac{1}{2}(X_2 + iY_2). \quad (12)$$

The detection stage of the interferometer consists of measuring the difference photocurrent $\hat{\mathcal{D}}_\eta = \mathcal{J}_{1,\eta} - \mathcal{J}_{2,\eta}$ between the outputs modes. Assuming photodetectors with equal quantum efficiency on the two modes, we have the mean value

$$\begin{aligned}\mathcal{D}_\eta &= \eta\langle a_1^\dagger a_1 - a_2^\dagger a_2\rangle \\ &= \eta\,{\rm Tr}[\varrho_{\rm out}(a_1^\dagger a_1 - a_2^\dagger a_2)] = \eta\langle[a_1^\dagger a_1]_{\rm s} - [a_2^\dagger a_2]_{\rm s}\rangle,\end{aligned} \quad (13)$$

$[\ldots]_{\rm s}$ denoting (Weyl) symmetric ordering, $\mathcal{D}_\eta = {\rm Tr}[\varrho_{\rm out}\hat{\mathcal{D}}_\eta]$, and variance [13]:

$$\Delta\mathcal{D}_\eta^2 = \eta^2\Delta\mathcal{D}_1^2 + \eta(1-\eta)N_{\rm tot}, \quad (14)$$

where $N_{\rm tot} = \langle a_1^\dagger a_1 + a_2^\dagger a_2\rangle$ and

$$\Delta\mathcal{D}_1^2 = \langle [a_1^{\dagger 2} a_1^2]_{\rm s}\rangle + \langle [a_2^{\dagger 2} a_2^2]_{\rm s}\rangle - \langle [a_1^\dagger a_1]_{\rm s}\rangle^2 - \langle [a_2^\dagger a_2]_{\rm s}\rangle^2 - 2\langle [a_1^\dagger a_1]_{\rm s}[a_2^\dagger a_2]_{\rm s}\rangle + 2\langle [a_1^\dagger a_1]_{\rm s}\rangle\langle [a_2^\dagger a_2]_{\rm s}\rangle - 1/2. \quad (15)$$

Since the displacement operator on mode h can be written as

$$D_h(\lambda) = \sum_{k,l=0}^{\infty} \frac{\lambda^k(\lambda^*)^l}{k!l!}[a_h^{\dagger k} a_h^l]_{\rm s}, \quad (16)$$

we have

$$[a_h^{\dagger n} a_h^m]_{\rm s} = \partial_\lambda^n \partial_{\lambda^*}^m D_h(\lambda)|_{\lambda=0}. \quad (17)$$

Besides, since

$$\chi(\lambda_1, \lambda_2) = {\rm Tr}[\varrho_{\rm out} D_1(\lambda_1) D_2(\lambda_2)], \quad (18)$$

we obtain

$$\langle [a_1^\dagger a_1]_{\rm s}\rangle = -\partial_{\lambda_1}\partial_{\lambda_1^*}\chi(\lambda_1, \lambda_2)|_{\lambda_1=\lambda_2=0}, \quad (19a)$$

$$\langle [a_2^\dagger a_2]_{\rm s}\rangle = -\partial_{\lambda_2}\partial_{\lambda_2^*}\chi(\lambda_1, \lambda_2)|_{\lambda_1=\lambda_2=0}, \quad (19b)$$

$$\langle [a_1^\dagger a_1]_{\rm s}[a_2^\dagger a_2]_{\rm s}\rangle = -\partial_{\lambda_1}\partial_{\lambda_1^*}\partial_{\lambda_2}\partial_{\lambda_2^*}\chi(\lambda_1, \lambda_2)|_{\lambda_1=\lambda_2=0}, \quad (19c)$$

$$\langle [a_1^{\dagger 2} a_1^2]_{\rm s}\rangle = \partial_{\lambda_1}^2\partial_{\lambda_1^*}^2\chi(\lambda_1, \lambda_2)|_{\lambda_1=\lambda_2=0}, \quad (19d)$$

$$\langle [a_2^{\dagger 2} a_2^2]_{\rm s}\rangle = \partial_{\lambda_2}^2\partial_{\lambda_2^*}^2\chi(\lambda_1, \lambda_2)|_{\lambda_1=\lambda_2=0}. \quad (19e)$$

Using Eqs. (18) and (19), we can write

$$\langle [a_1^\dagger a_1]_{\rm s}\rangle = \mathcal{A} + |\mathcal{U}|^2, \quad (20a)$$

$$\langle [a_2^\dagger a_2]_{\rm s}\rangle = \mathcal{B} + |\mathcal{V}|^2, \quad (20b)$$

$$\langle [a_1^\dagger a_1]_{\rm s}[a_2^\dagger a_2]_{\rm s}\rangle = |\mathcal{E}|^2 + \mathcal{A}|\mathcal{V}|^2 + \mathcal{B}|\mathcal{U}|^2 + |\mathcal{U}|^2|\mathcal{V}|^2 + |\mathcal{F}|^2 + \mathcal{A}\mathcal{B} + \mathcal{U}^*\mathcal{V}^*\mathcal{E} + \mathcal{U}\mathcal{V}\mathcal{E}^* + \mathcal{V}^*\mathcal{U}\mathcal{F} + \mathcal{F}^*\mathcal{U}^*\mathcal{V}, \quad (20c)$$

$$\langle [a_1^{\dagger 2} a_1^2]_{\rm s}\rangle = 2\mathcal{A}^2 + 4\mathcal{A}|\mathcal{U}|^2 + \left|2\mathcal{E} + \mathcal{U}^2\right|^2, \quad (20d)$$

$$\langle [a_2^{\dagger 2} a_2^2]_{\rm s}\rangle = 2\mathcal{B}^2 + 4\mathcal{B}|\mathcal{V}|^2 + \left|2\mathcal{D} + \mathcal{V}^2\right|^2. \quad (20e)$$

$\mathcal{D}_\eta$ and its variance $\Delta\mathcal{D}_\eta^2$ depend only on the covariance matrix $\boldsymbol{\sigma}_{\rm out}$ and $\mathbf{X}_{\rm out}$ as expected, since the output state is still Gaussian.

3. SENSITIVITY

Let us assume two squeezed states as input states, i.e., $\varrho_{\rm in} = |\psi_{\rm in}\rangle\langle\langle\psi_{\rm in}|$, with $|\psi_{\rm in}\rangle\rangle = |\alpha, \xi\rangle_{\rm s} \otimes |\gamma, \zeta\rangle_{\rm p}$, where, e.g., $|\alpha, \xi\rangle = D(\alpha)S(\xi)|0\rangle$, $D(\alpha)$ and $S(\xi)$ being the displacement and the squeezing operator, respectively, and the subscript "s" and "p" refer to "signal" and "probe" as well, as in Fig. 1. In the following we suppress these subscripts, being clear from the context what is the signal and what the probe. The covariance matrix of the two mode input state reads [see Eq. (1)]:

$$\boldsymbol{\sigma}_{\rm in} = \left(\begin{array}{c|c} \mathbf{S}_\xi & \mathbf{0} \\ \hline \mathbf{0} & \mathbf{S}_\zeta \end{array}\right), \quad (21)$$

where

$$\mathbf{S}_\chi = \frac{1}{2}\begin{pmatrix} f_+(\chi) & g(\chi) \\ g(\chi) & f_-(\chi) \end{pmatrix}, \quad \chi = \xi, \zeta, \quad (22)$$

with

$$f_\pm(\chi) = \cosh(2|\chi|) \pm \sinh(2|\chi|)\cos({\rm arg}[\chi]), \quad (23)$$

$$g(\chi) = -\sinh(2|\chi|)\sin({\rm arg}[\chi]), \quad (24)$$

and

$$\mathbf{X}_{\rm in}^T = \sqrt{2}\,({\rm Re}[\alpha], {\rm Im}[\alpha], {\rm Re}[\alpha], {\rm Im}[\alpha]).$$

For the sake of simplicity and without loss of generality, we can assume $\alpha, \xi \in \mathbb{R}$, $\zeta = re^{-i\theta}$, with $r \in \mathbb{R}$, and we put $\gamma = 0$. In turn, the total number of photon of the input state is

$$N_{\rm tot} = |\alpha|^2 + \beta_{\rm tot} N_{\rm tot}, \quad (25)$$

where $\beta_{\rm tot} \equiv \beta_\xi + \beta_\zeta$ and we defined the squeezing fractions $\beta_x = (\sinh^2|x|)/N_{\rm tot}$, $x = \xi, \zeta$.

3.1. Ideal Detection

First of all, we assume a perfect detection at the interferometer outputs, i.e., $\eta = 1$. In this case the sensitivity $\mathcal{S}_1 \equiv \mathcal{S}_1(N_{\rm tot}, \beta_{\rm tot}, \beta_\zeta)$ of the interferometer is defined as

$$\mathcal{S}_1 = \sqrt{\Delta\mathcal{D}_1^2}/|\partial_\phi \mathcal{D}_1|, \quad (26)$$

where $\Delta\mathcal{D}_1^2$ is given in Eq. (15). In general, the analytic expression of Eq. (26) is quite cumbersome, so we do not report it explicitly, but we address the results obtained in some specific case. First of all, we optimize the relative phase between the two squeezed states in order to minimize the sensitivity (26). In Fig. 2 we plot the sensitivity $\mathcal{S}_1$ of the MZ interferometer for the input state $|\alpha, \xi\rangle \otimes |\beta, \zeta\rangle$ as a function of the phase shift ϕ and

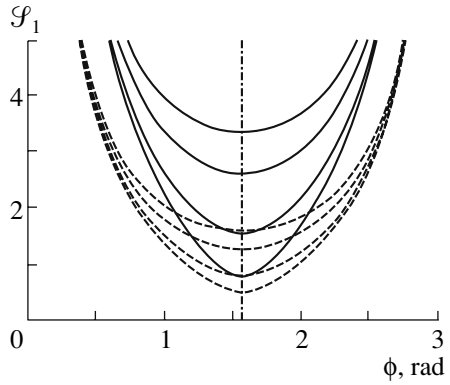

Fig. 2. Plot of the sensitivity $\mathcal{S}_1$ of the MZ interferometer for the input state $|\alpha, \xi\rangle \otimes |\beta, \zeta\rangle$ with $\alpha = 1$, $\beta = 0$, and $\xi = 0.7$, $\zeta = 0.5e^{i\theta}$ (dashed lines), or $\xi = 0.5$, $\zeta = 0.7e^{i\theta}$ (solid lines), as a function of the MZ phase shift ϕ and different values of θ, from bottom to top: $\theta = 0$, $\pi/4$, $\pi/2$, and $3\pi/4$. The vertical dash-dotted line is $\phi = \pi/2$.

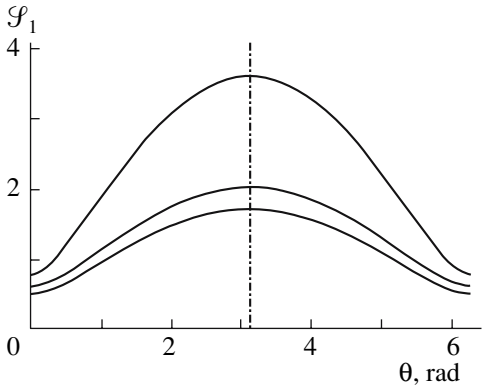

Fig. 3. Plot of the sensitivity $\mathcal{S}_1$ of the MZ interferometer with $\phi = \pi/2$ for the input state $|\alpha, \xi\rangle \otimes |\beta, |\zeta|e^{i\theta}\rangle$ as a function of θ. We put $\alpha = 1$, $\beta = 0$, and, from top to bottom: $\xi = 0.5$, and $\zeta = 0.7e^{i\theta}$; $\xi = 0.5$, and $\zeta = 0.5e^{i\theta}$; $\xi = 0.7$, and $\zeta = 0.5e^{i\theta}$. The vertical dash-dotted line is $\theta = \pi/2$.

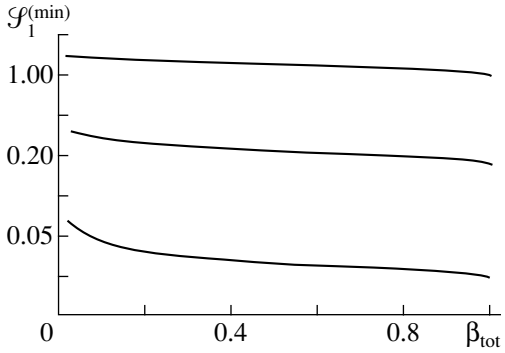

Fig. 4. Logarithmic plot of the minimum $\mathcal{S}_1^{(\min)}$ of the sensitivity (i.e., optimized with respect to β_ζ) as a function of the total squeezing fraction β_{tot} with $\phi = \pi/2$, and $\theta = 0$, and different values of N_{tot}, from top to bottom: $N_{tot} = 0.5$, 5, and 50.

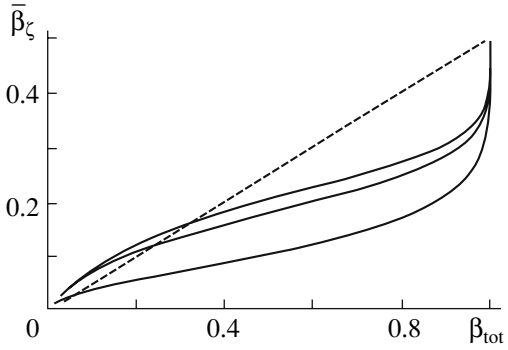

Fig. 5. Plot of the signal squeezing fraction $\bar{\beta}_\zeta$ for which the minimum of the sensitivity is achieved in ideal case, i.e., $\eta = 1$, as a function of the total squeezing fraction β_{tot}. We set $\phi = \pi/2$, $\theta = 0$ and, from top to bottom (solid lines) $N_{tot} = 50$, 5, and 0.5. The dashed line refers to $\bar{\beta}_\zeta = \beta_{tot}/2$.

different values of the squeezing phase θ. We can see that the minimum of the sensitivity is achieved for $\phi = \pi/2$ and $\theta = 0$, i.e., the signal and the probe should be squeezed in the same direction (see also Fig. 3). From now on, we will assume $\phi = \pi/2$ and $\theta = 0$ as working regime. Figure 4 refers to the minimum value $\mathcal{S}_1^{(\min)} \equiv \mathcal{S}_1^{(\min)}(N_{tot}, \beta_{tot})$, where

$$\mathcal{S}_1^{(\min)}(N_{tot}, \beta_{tot}) = \min_{\beta_\zeta \in [0, \beta_{tot}]} \{\mathcal{S}_1(N_{tot}, \beta_{tot}, \beta_\zeta)\} \quad (27)$$

of the sensitivity as a function of β_{tot} and different values of the total number of photons N_{tot}: we find that squeezing the input states is always convenient, at least in the ideal case, even if the improvement of the sensitivity actually depends on the ratio β_ξ/β_ζ. This is investigated in Fig. 5, where the optimal squeezing probe fraction $\bar{\beta}_\zeta$, which minimizes the sensitivity, is plotted as a function of β_{tot}. For a given N_{tot}, there exists a threshold value on β_{tot} under which the probe should be more squeezed than the signal in order to minimize $\mathcal{S}$. On the other hand, as β_{tot} approaches 1, the squeezing should be equally distributed between signal and probe.

Let us now address the dependence of the sensitivity on the total number of photons N_{tot}. In the absence of any squeezing, i.e., $\beta_{tot} = 0$, Eq. (26) reduces to

$$\mathcal{S}_1(N_{tot}, 0, 0) = 1/\sqrt{N_{tot}}, \quad (28)$$

which corresponds to the $1/\sqrt{N_{tot}} \equiv \mathcal{S}_{PC}$ photon-counting statistics limit due to the unavoidable fluctuations in number of output photons [1]. As pointed out in [2], by using the "squeezing" resource, one can reduce the

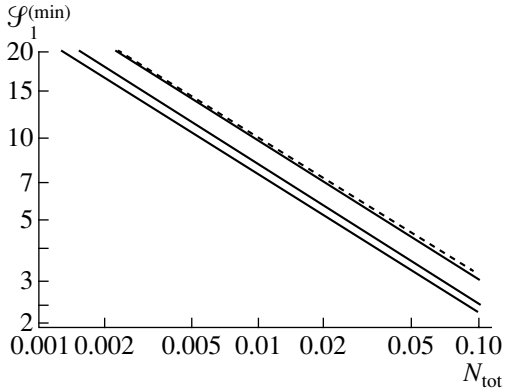

Fig. 6. (Low-energy regime) Bilogarithmic plot of the minimum (i.e., optimized with respect to β_ζ) sensitivity $\mathcal{S}_1^{(\min)}$ as a function of $N_{\rm tot}$ for different values of the total squeezing fraction, from top to bottom (solid lines): $\beta_{\rm tot} = 0.1$, 0.9, and 0.99. The dashed line refers to $\mathcal{S}_1^{(\min)} = (\sqrt{N_{\rm tot}})^{-1}$.

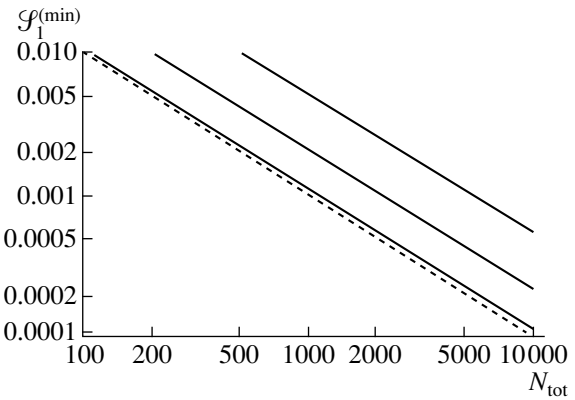

Fig. 7. (High-energy regime) Bilogarithmic plot of the minimum (i.e., optimized with respect to β_ζ) sensitivity $\mathcal{S}_1^{(\min)}$ as a function of $N_{\rm tot}$ for different values of the total squeezing fraction, from top to bottom (solid lines): $\beta_{\rm tot} = 0.01$, 0.1, and 0.9. The dashed line refers to $\mathcal{S}_1^{(\min)} = (N_{\rm tot})^{-1}$.

counting-photon error. This is explicitly shown in Figs. 6 and 7 in the case of low- and high-energy regimes, respectively. When $N_{\rm tot} \ll 1$ (low-energy regime), we have $\mathcal{S}_1^{(\min)} \propto (\sqrt{N_{\rm tot}})^{-1}$. We do not report the analytic expression of the sensitivity in this limit since it is quite cumbersome. However, one finds that squeezing the input states gives a better sensitivity then $\mathcal{S}_{\rm PC}$ (see Fig. 6). In the limit $N_{\rm tot} \gg 1$ (high-energy regime) we have

$$\mathcal{S}_1^{(\min)} \approx \frac{1}{2N_{\rm tot}} \frac{1}{|1-2\beta_\zeta|} \sqrt{\frac{1}{\beta_\zeta} + \frac{\beta_\zeta}{\beta_{\rm tot}-\beta_\zeta} - 3}. \qquad (29)$$

In Fig. 7 we plot $\mathcal{S}_1^{(\min)}$ as a function of $N_{\rm tot}$ and different values of the total squeezing fraction; it is evident that $\mathcal{S}_1^{(\min)} \propto (\sqrt{N_{\rm tot}})^{-1}$.

3.2. Real Detectors

So far, we have addressed the case in which the efficiency of the detectors are taken as equal to 1. Indeed, if the detectors are affected by losses (nonunit quantum efficiency), the sensitivity of the interferometer becomes worse (i.e., its actual value becomes larger than the ideal case). This can be easily seen writing the nonideal sensitivity $\mathcal{S}_\eta \equiv \mathcal{S}_\eta(N_{\rm tot}, \beta_{\rm tot}, \beta_\zeta)$ as follows:

$$\mathcal{S}_\eta = \mathcal{S}_1 \sqrt{1 + (1-\eta) N_{\rm tot}/\eta \Delta\mathcal{D}_1^2}, \qquad (30)$$

where $\mathcal{S}_1$ is the same as in Eq. (26). If $\beta_{\rm tot} = 0$ we have

$$\mathcal{S}_\eta(N_{\rm tot}, 0, 0) = 1/\sqrt{\eta N_{\rm tot}}. \qquad (31)$$

In the low-energy regime (i.e., $N_{\rm tot} \ll 1$) and in the presence of squeezing (i.e., $\beta_{\rm tot} \neq 0$), Eq. (30) gives

$$\mathcal{S}_\eta \approx \frac{1}{|1-2\beta_\zeta|} \sqrt{\frac{1 - 2\eta\sqrt{\beta_\zeta(\beta_{\rm tot}-\beta_\zeta)}}{\eta N_{\rm tot}}}. \qquad (32)$$

If $N_{\rm tot} \gg 1$ (high-energy regime) and $\beta_{\rm tot} \neq 0$, then we have

$$\mathcal{S}_\eta \approx \frac{1}{|1-2\beta_\zeta|} \sqrt{\frac{1-\eta}{\eta N_{\rm tot}}}. \qquad (33)$$

In Figs. 8 and 9 we plot $\mathcal{S}_\eta^{(\min)}$, defined as follows:

$$\mathcal{S}_\eta^{(\min)}(N_{\rm tot}, \beta_{\rm tot}) = \min_{\beta_\zeta \in [0, \beta_{\rm tot}]} \{\mathcal{S}_\eta(N_{\rm tot}, \beta_{\rm tot}, \beta_\zeta)\} \qquad (34)$$

in the regimes of low and high energy, respectively, for different values of the other involved parameters; the

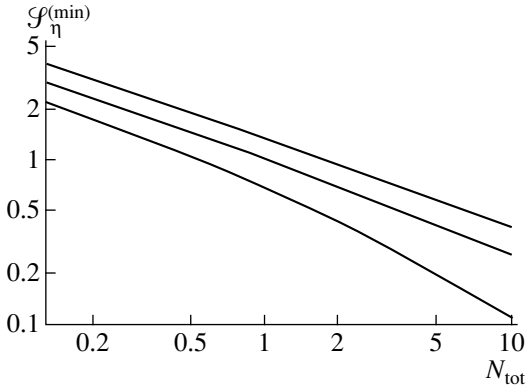

Fig. 8. (Low-energy regime) Bilogarithmic plot of the minimum (i.e., optimized with respect to β_ζ) sensitivity $\mathcal{S}_\eta^{(\min)}$ as a function of $N_{\rm tot}$ with $\beta_{\rm tot} = 0.8$ and different values of η, from bottom to top: $\eta = 1.0$, 0.75, and 0.5.

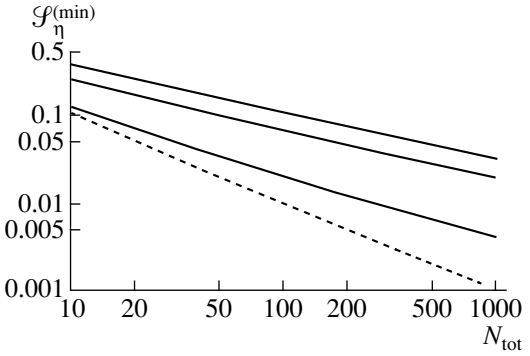

Fig. 9. (High-energy regime) Bi-logarithmic plot of the minimum (i.e., optimized with respect to β_ζ) sensitivity $\mathcal{S}_\eta^{(\min)}$ as a function of $N_{\rm tot}$ with $\beta_{\rm tot} = 0.8$ and different values of η, from bottom to top (solid lines): $\eta = 1.0$, 0.75, and 0.5. The dashed line refers to $\mathcal{S}_\eta^{(\min)} = (N_{\rm tot})^{-1}$.

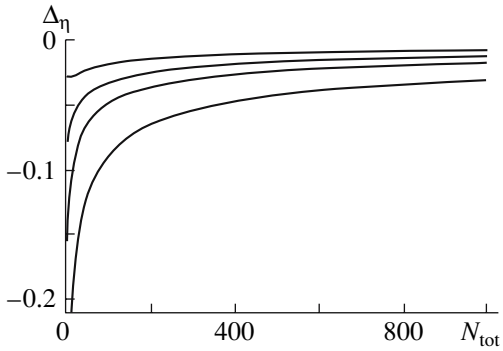

Fig. 10. Plot of $\Delta_\eta(N_{\rm tot}, \beta_{\rm tot})$ as a function of $N_{\rm tot}$ with $\beta_{\rm tot} = 0.8$ and different values of η, from bottom to top (solid lines): $\eta = 1.0$, 0.75, 0.5, and 0.25.

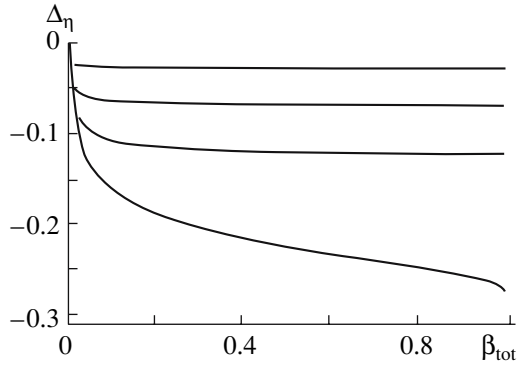

Fig. 11. Plot of $\Delta_\eta(N_{\rm tot}, \beta_{\rm tot})$ as a function of $\beta_{\rm tot}$ with $N_{\rm tot} = 5$ and different values of η, from bottom to top (solid lines): $\eta = 1.0$, 0.75, 0.5, and 0.25.

behavior $(N_{\rm tot})^{-1/2}$ is evident. Notice that the asymptotic value (32) does not depend on the total squeezing fraction (even if one should have $\beta_{\rm tot} \neq 0$) but only on β_ζ. Even if in the presence of a nonunit quantum efficiency, one loses the dependence $(N_{\rm tot})^{-1}$ given in Eq. (29), it is possible to choose the squeezing fraction β_ζ in Eq. (32) in order to have a better sensitivity (a smaller value) than the one in Eq. (31). In particular, in Fig. 10, where we plot the difference

$$\Delta_\eta(N_{\rm tot}, \beta_{\rm tot}) = \mathcal{S}_\eta^{(\min)}(N_{\rm tot}, \beta_{\rm tot}) - \mathcal{S}_\eta(N_{\rm tot}, 0, 0) \quad (35)$$

as a function of $N_{\rm tot}$ for different values of η and $\beta_{\rm tot} = 0.8$, we can see that "squeezing" the input is always convenient in optimal conditions, namely, after the minimization of sensitivity; in fact in this case one has always $\Delta_\eta(N_{\rm tot}, \beta_{\rm tot}) < 0$, i.e.,

$$\mathcal{S}_\eta^{(\min)}(N_{\rm tot}, \beta_{\rm tot}) < \mathcal{S}_\eta(N_{\rm tot}, 0, 0).$$

This result does not change if we vary the total squeezing fraction, as one can conclude from Fig. 11.

4. CONCLUDING REMARKS

By means of a suitable phase-space description, we have optimized the sensitivity of the MZ interferometer when the input states are two squeezed coherent states. The working regime of the interferometer has been optimized at fixed input energy versus the squeezing phases and amplitudes, as well as the distribution of squeezing in the two input signals. Our analysis has been carried out without particular assumptions on the input states total energy or squeezing. For ideal detection we have found the known result that the squeezing resource allows to beat the shot-noise limit; for nonunit detection efficiency, we have shown that for fixed input energy one can always optimize the squeezing fraction between the input states in order to enhance the sensitivity with respect to the case of no squeezing. However, in these last cases one cannot go beyond the shot-noise limit.

ACKNOWLEDGMENTS

This work has been supported by MIUR through the project PRIN-2005024254-002.

REFERENCES

1. C. M. Caves, Phys. Rev. Lett. **45**, 75 (1980).
2. C. M. Caves, Phys. Rev. D **23**, 1693 (1981).
3. R. S. Bondurant and J. H. Shapiro, Phys. Rev. D **30**, 2548 (1984).
4. M. G. A. Paris, Phys. Lett. A **201**, 132 (1995).
5. A. Luis, Phys. Rev. A **69**, 045801 (2004).
6. Z. Hradil et al., Phys. Rev. Lett. **76**, 4295 (1996).
7. M. Zawisky et al., J. Phys. A **31**, 551 (1998).
8. M. G. A. Paris, Phys. Lett. A **225**, 23 (1997).
9. J. Řeháček, et al., Phys. Rev. A **60**, 473 (1999).
10. L. Pezzé and A. Smerzi, Phys. Rev. A **73**, 011801(R) (2006).
11. L. Pezzé and A. Smerzi, Europhysics Letters **78**, 30004 (2007).
12. A. Ferraro, S. Olivares, and M. G. A. Paris, *Gaussian States in Quantum Information* (Bibliopolis, Napoli, 2005).
13. A. Agliati, M. Bondani, A. Andreoni, et al., J. Opt. B. **7**, 652 (2005).